Science Advances

AAAS

advances.sciencemag.org/cgi/content/full/3/6/e1603001/DC1

Supplementary Materials for

Serotonin rebalances cortical tuning and behavior linked to autism symptoms in 15q11-13 CNV mice

Nobuhiro Nakai, Masatoshi Nagano, Fumihito Saitow, Yasuhito Watanabe, Yoshinobu Kawamura, Akiko Kawamoto, Kota Tamada, Hiroshi Mizuma, Hirotaka Onoe, Yasuyoshi Watanabe, Hiromu Monai, Hajime Hirase, Jin Nakatani, Hirofumi Inagaki, Tomoyuki Kawada, Taisuke Miyazaki, Masahiko Watanabe, Yuka Sato, Shigeo Okabe, Kazuo Kitamura, Masanobu Kano, Kouichi Hashimoto, Hidenori Suzuki, Toru Takumi

Published 21 June 2017, *Sci. Adv.* **3**, e1603001 (2017)
DOI: 10.1126/sciadv.1603001

This PDF file includes:

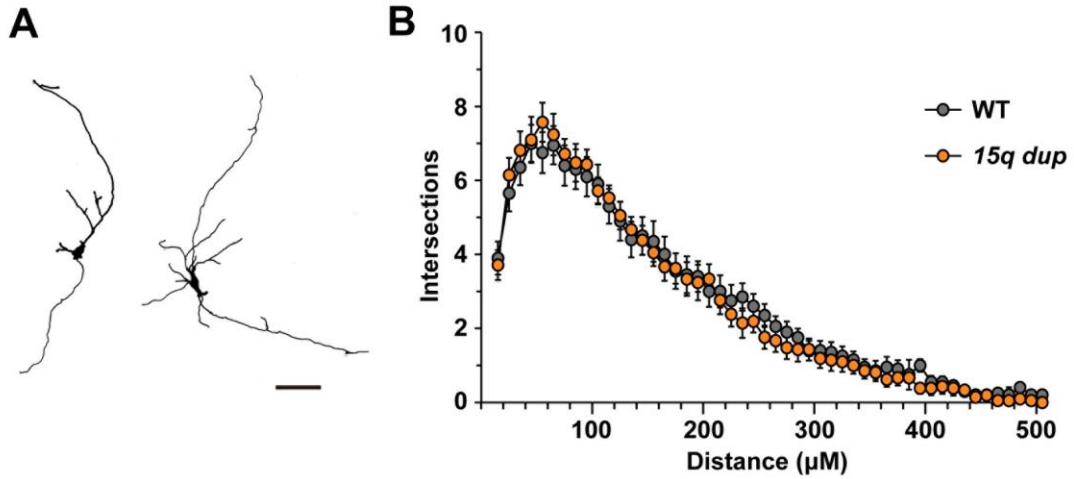

fig. S1. Dendritic morphology of lwDRN 5-HT neurons shows no difference between WT and *15q dup* mice. (**A**) Representative tracings demonstrate morphologies of lwDRN 5-HT neurons obtained from wild-type (WT) mouse neurons reconstituted by biocytin-labeling identification of recorded cells. Scale bar, 100 μm. (**B**) The dendritic tree complexity was quantified by Sholl analysis, revealing that the lwDRN neurons did not differ between genotypes ($P = 0.11$; two-sample Kolmogorov–Smirnov test; WT: 20 neurons from 4 mice, *15q dup*: 21 neurons from 4 mice). Error bars indicate mean±SEM.

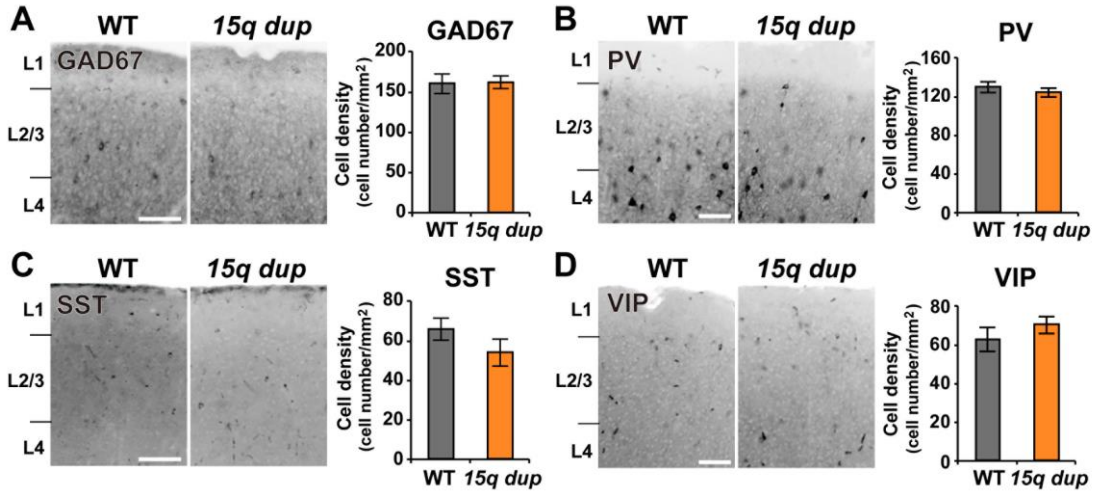

fig. S2. Cell densities of inhibitory neurons are unchanged in *15q dup* mice. (**A** to **D**) Representative images of immunohistochemistry of inhibitory neuronal markers and the quantification of the immunostained cells in L2/3 of S1BF. There were no differences in cell densities of (A) glutamic acid decarboxylase 67 kDa isoform (GAD67), (B) parvalbumin (PV), (C) somatostatin (SST) and (D) vasoactive intestinal peptide (VIP)-expressing cells between genotypes. WT: (A,C) *n* = 12 sections from 4 mice, (B, D) *n* = 30 sections from 5 mice; *15q dup*: (A,C) *n* = 15 sections from 5 mice, (B, D) *n* = 30 sections from 5 mice. Scale bar, 200 μm. Error bars indicate mean±SEM.

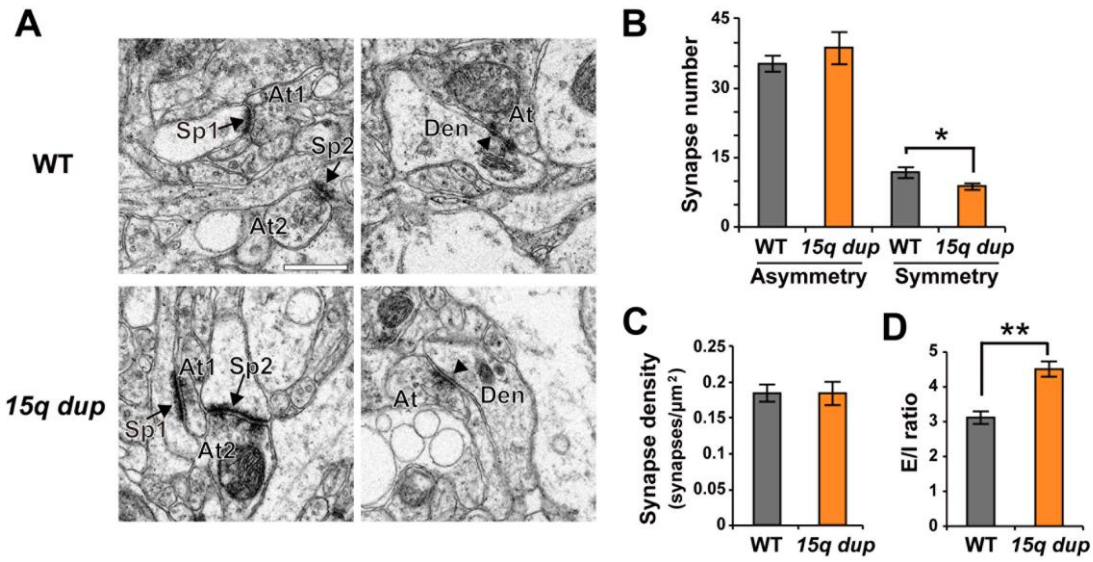

fig. S3. The number of symmetry synapses is decreased in the S1BF of *15q dup* mice. (**A**) Representative EM micrograph show asymmetric and symmetric synapses taken at a magnification of 5,000× at 50 μm depth from surface of S1BF in WT (upper) and *15q dup* mice (bottom). Arrows indicate asymmetric synapse and arrowheads indicate symmetric synapse. At, axon terminal; Sp, spine; Den, dendrite. Scale bar, 0.5 μm. (**B**) The number of symmetry synapse, which indicates inhibitory synapse, was fewer in *15q dup* mice, while the number of asymmetry synapse, which indicates excitatory synapse, was not changed. (**C**) There was no difference in synapse density between genotypes. (**D**) The E/I ratio represented by asymmetry/symmetry synapse was increased in *15q dup* mice. (n = 6 sections from two mice in each genotype, *P < 0.05, **P < 0.001, one-tailed t-test). Error bars indicate mean±SEM.

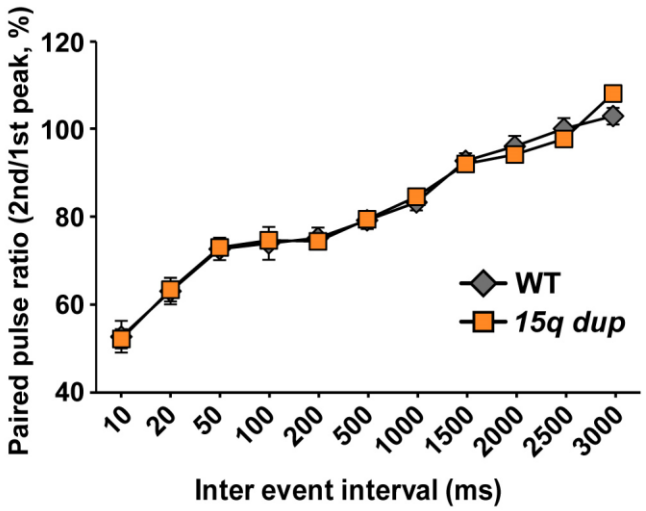

fig. S4. The paired-pulse ratio of inhibitory transmissions in S1BF L2/3 pyramidal neurons is not changed in *15q dup* mice. The graph shows the paired-pulse ratio (PPR) of evoked IPSCs (eIPSCs) at 10 to 3000 ms inter-event intervals. Evoked IPSCs were elicited by local stimulation of inhibitory inputs with a glass microelectrode placed around a given L2/3 pyramidal neuron. PPR was comparable between the genotypes, indicating that inhibitory synapses in *15q dup* mice have a normal release probability. WT: n = 8 from 4 mice, *15q dup*: n = 12 from 4 mice. Error bars indicate mean±SEM.

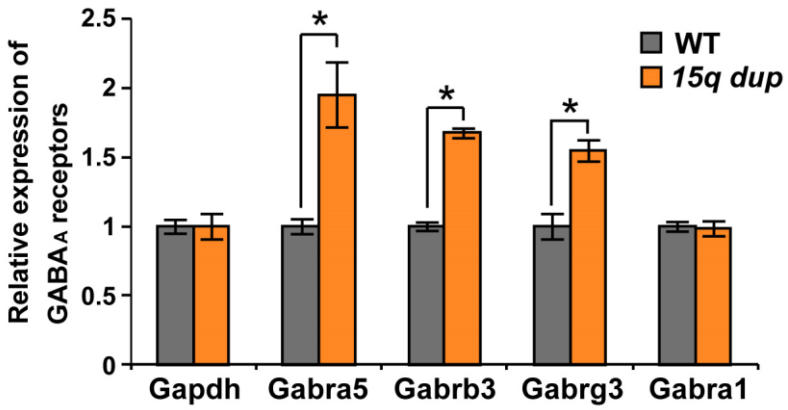

fig. S5. *15q dup* S1BF have differential expression of GABA$_A$ receptor subunits. Quantitative gene expression of GABA$_A$ receptor subunits in S1BF at P21 male mice. Gene expression was normalized by *Gapdh* expression in each sample. The graph shows the fold change relative to the gene expression in WT mice. The expression of *Gabra5*, *Gabrb3*, and *Gabrg3* were increased, but *Gabra1* was not changed. WT: $n = 4$ mice from two litters, *15q dup*: $n = 5$ mice from two litters. $^*P < 0.05$, Welch's *t*-test with Holm's correction. Error bars indicate mean±SEM.

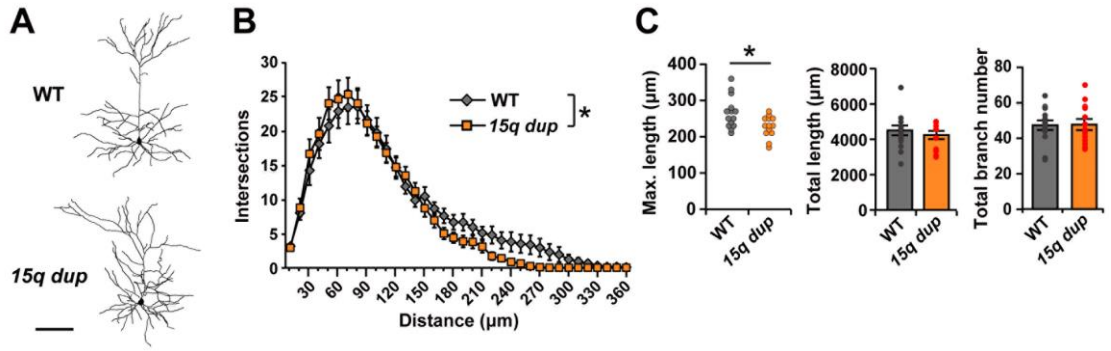

fig. S6. *15q dup* mice have decreased dendritic length of S1BF L2/3 pyramidal neurons. (**A**) Representative reconstruction images of L2/3 pyramidal neuron in S1BF of WT and *15q dup* mice. Scale bar, 100 μm. (**B**) The complexity of dendritic branches was analyzed by counting the crossing of concentric circles by the dendrites. The crossings of dendrites in distant areas from the soma were decreased in *15q dup* mice, compared to WT mice. Two-way repeated measures ANOVA showed a significant difference between genotypes (genotype: $F_{1, 35} = 5.596$, $^*P < 0.05$; there was no interaction between number of crossing and genotype). (**C**) The maximum apical dendrite length was shorter in *15q dup* pyramidal neurons ($^*P < 0.05$, Wilcoxon rank sum test), but the total length and the branch number of dendrites of pyramidal neurons were comparable between genotypes. WT: $n = 14$ cells from 7 mice, *15q dup*: $n = 13$ from 4 mice. Error bars indicate mean±SEM.

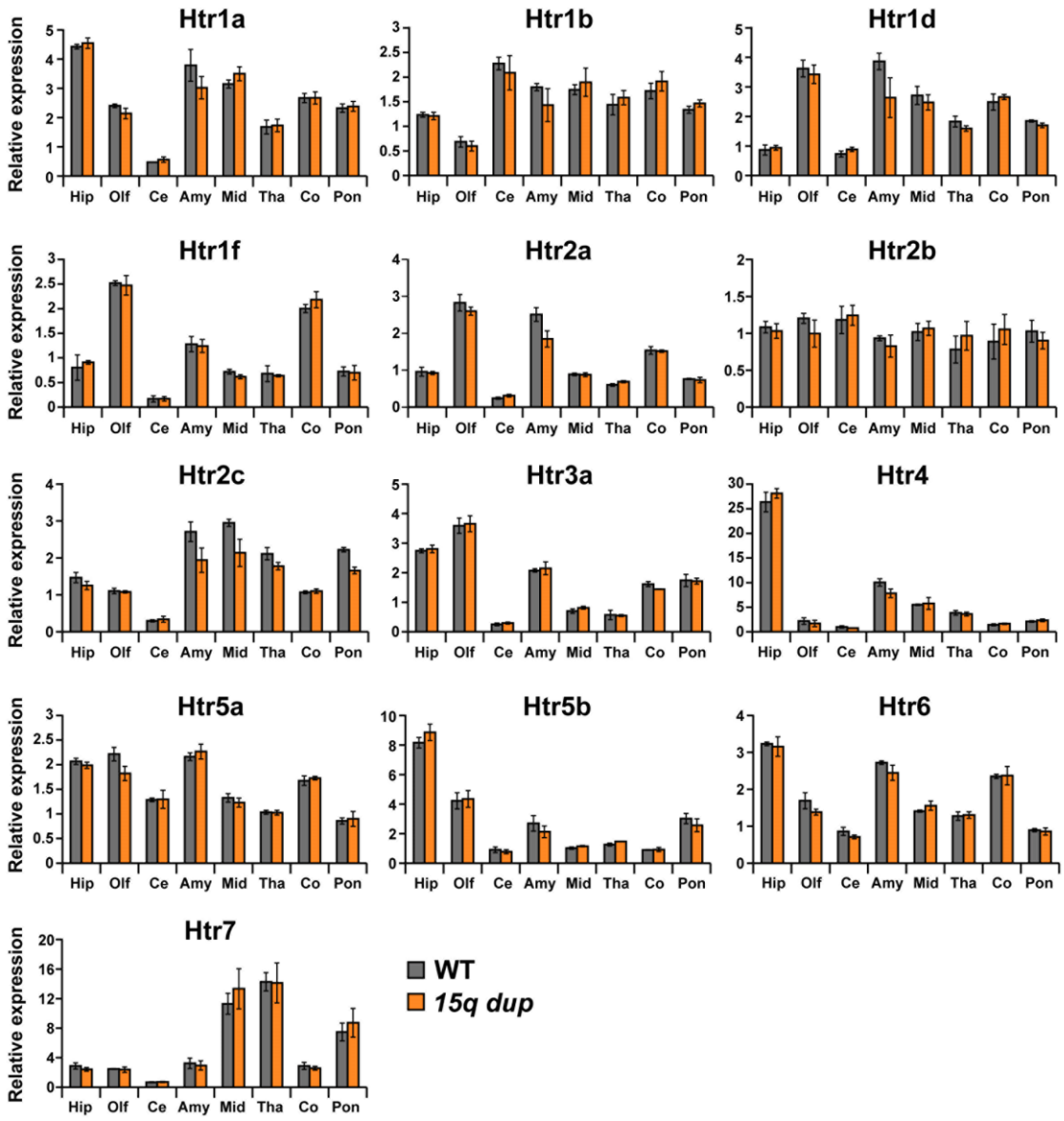

fig. S7. Profiling of 5-HT receptor expression in *15q dup* brain. The gene expression of 5-HT receptors was measured by qPCR. The brain from P14 male mice was sampled and separated to 8 regions. The relative expression of 5-HT receptors was normalized by *Gapdh* expression at each sample. There was no difference in each 5-HT receptors between genotypes (n = 3 mice from two litters in each genotype). Hip: hippocampus, Olf: olfactory bulb, Ce: cerebellum, Amy: amygdara, Mid: midbrain, Tha: thalamus and hypothalamus, Co: cortex, Pon: pons and medulla. Error bars indicate mean±SEM.

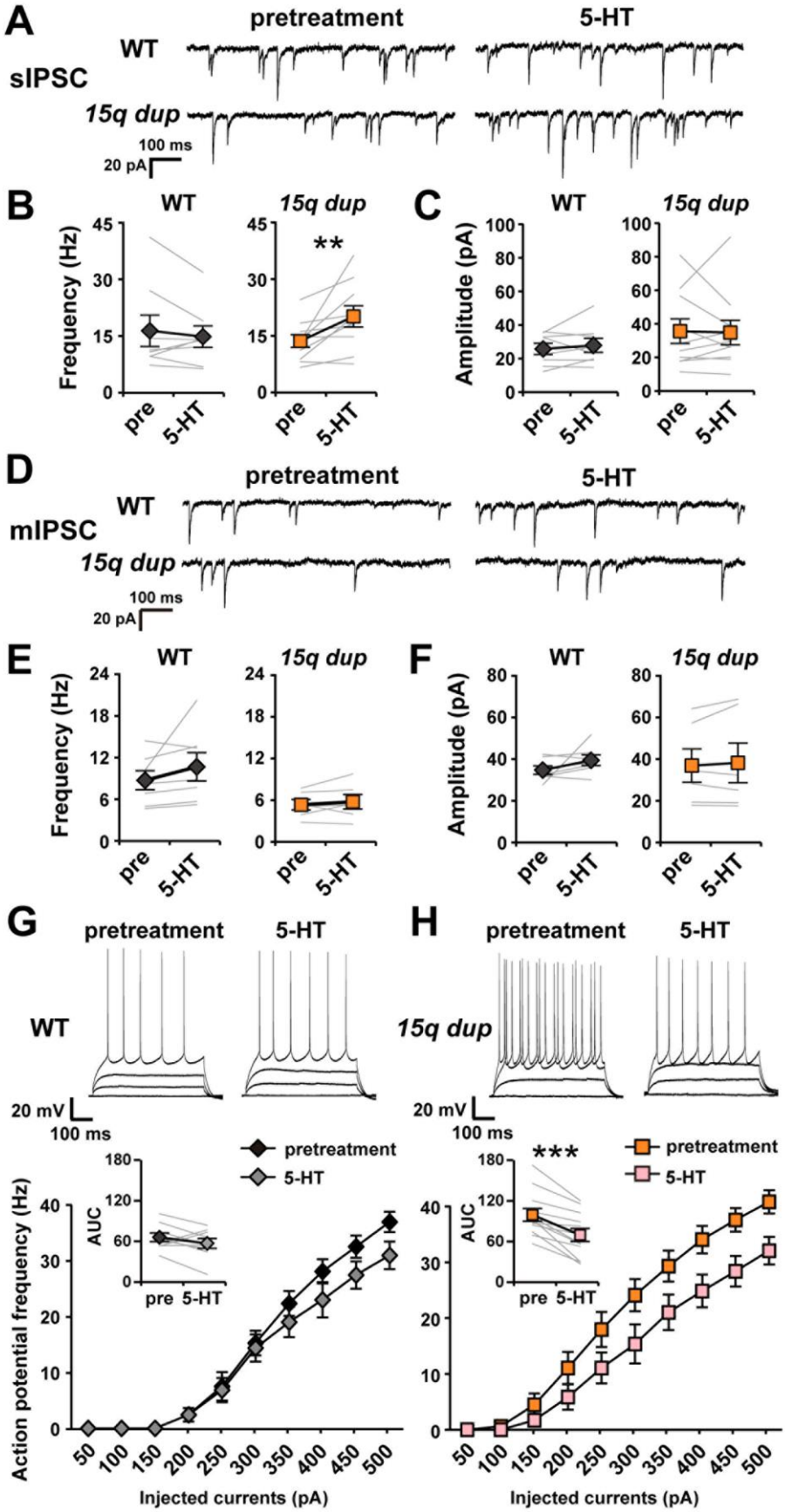
A
pretreatment
5-HT
WT
sIPSC
15q dup
100 ms
20 pA
B
WT
15q dup
Frequency (Hz)
**
pre
5-HT
C
Amplitude (pA)
D
mIPSC
E
F
G
pretreatment
5-HT
WT
20 mV
100 ms
pretreatment
5-HT
AUC
Action potential frequency (Hz)
Injected currents (pA)
H
15q dup
***

fig. S8. Acute 5-HT application enhances inhibitory transmission and suppresses excitability of S1BF L2/3 pyramidal neurons in *15q dup* mice. (**A**) Representative traces of sIPSCs at the conditions of pretreatment and 5-HT treatment. The sIPSCs were recorded from same L2/3 pyramidal neuron in the S1BF of WT and *15q dup* mice. (**B**) Comparison between sIPSCs frequencies of pretreatment and 5-HT treatment. The frequency in *15q dup* mice was increased by 5-HT, while the frequency in WT mice was not changed (***P* < 0.01, Exact Wilcoxon signed rank test). (**C**) The 5-HT treatment did not affect the amplitude of sIPSCs in both genotypes. WT: *n* = 8 neurons from 7 mice, *15q dup*: *n* = 10 from 8 mice. (**D**) Representative traces of mIPSCs at the conditions of pretreatment and 5-HT treatment. (**E** and **F**) The 5-HT treatment did not change the mIPSCs frequency and amplitude in both genotypes. WT: *n* = 7 neurons from 3 mice, *15q dup*: *n* = 6 from 3 mice. (**G** and **H**) Representative voltage traces in response to hyperpolarizing and depolarizing current injections at the conditions of pretreatment and 5-HT treatment in L2/3 pyramidal neurons of S1BF. In WT neurons, 5-HT did not change action potential frequency (G) while 5-HT suppressed action potential frequency in *15q dup* neurons (H, ****P* < 0.001, two-tailed paired *t*-test). WT: *n* = 9 neurons from 3 mice, *15q dup*: *n* = 12 from 4 mice. AUC: the area under the curve in line graph. In all panels error bars indicate mean±SEM.

table S1. Properties of action potentials of 5-HT neurons in DRN.

Age: 5-8 weeks	**WT (n = 41 cells)**	***15q dup*** **(n = 47 cells)**
AP thre (mV)	-32.0 ± 0.64	-32.5 ± 0.64
AP half width (ms)	1.8 ± 0.08	1.8 ± 0.06
AP $_{AHP}$ (mV)	-17.1 ± 0.41	-16.8 ± 0.46

AP thre: threshold potential for action potential generation, AP $_{AHP}$: amplitude after hyperpolarization, AP half with: kinetics of action potential half-height width

table S2. Firing properties of L2/3 regular spiking neurons in vivo.

Age: P28-65	**WT (*n* = 28 cells)**	***15q dup* (*n* = 27 cells)**
Cell depth (μm)	274.5 ± 8.7	296.7 ± 11.8
Resting Vm (mV)	-79.4 ± 1.6	-76.9 ± 1.4
AP amp (mV)	72.7 ± 2.1	73.6 ± 2.0
AP half width (ms)	0.81 ± 0.02	0.82 ± 0.03
AP thre (mV)	-37.4 ± 1.2	-38.3 ± 1.2
AP freq (Hz)	0.08 ± 0.05	0.08 ± 0.03
Up-Down ΔV (mV)	14.0 ± 0.5	14.6 ± 0.4

AP amp: action potential amplitude, AP thre: action potential threshold, AP freq: action potential frequency, Up-Down ΔV: averaged Up state amplitude

table S3. Statistical results.

Figure	Sample type	Sample number				Normal distribution (No: at least more than one group)	Shapiro-Wilk normality test (WT, 15q) or (V-WT, V-15q, F-WT, F-15q)	F test or Bartlett test n.a.: not applicable	Statistics	Group	P value	Degrees of Freedom& F/t/z/R/ETC VALUE
		WT or Veh-WT	15q or Veh-15q	FLX-WT	FLX-15q							
Fig. 1B	cells/mice	83/8	105/8			No	0.04, 0.006	0.13	Wilcoxon rank sum test		0.006	W = 5384
Fig. 1D	cells/mice	60/8	62/9			No	0.008, 0.08	0.03	Brunner-Munzel test	Amp	0.048	t(118) = 2.00
						No	<0.001, <0.001	0.008		Freq	0.61	t(118) = 0.51
Fig. 1E	cells/mice	13/3	10/3			No	0.15, 0.04	0.10	Wilcoxon rank sum test	Amp	0.02	W = 103
						No	0.77, 0.03	0.40		Freq	0.45	W = 78
Fig. 1M	mice/litters	7/6	7/6			Yes	0.87, 0.57	0.54	two-tailed t-test	DRN	<0.001	t(12) = 6.20
						Yes	0.50, 0.24	0.59		Cg	<0.001	t(12) = 5.68
						Yes	0.62, 0.27	0.64		Hip	<0.001	t(12) = 5.41
Fig. 2C	mice/litters	9/4	9/4			Yes	0.07,0.26	0.12	Wilcoxon rank sum test	Principal	0.49	W = 32
						No	0.005, 0.02	0.17		Surround	0.007	W = 11
Fig. 2E						Yes	0.15, 0.79	0.62	two-tailed t-test		0.02	t(16) = 2.63
Fig. 2F						Yes	0.09, 0.67	0.32	two-tailed t-test		0.02	t(16) = 2.64
Fig. 2I	mice/litters	12/more than 5	16/more than 5			Yes	0.29, 0.99	0.76	two-tailed t-test	Principal	0.45	t(26) = 0.77
						Yes	0.80, 0.76	0.31		Surround	0.03	t(26) = 2.28
Fig. 2J						Yes	0.98, 0.60	0.16	two-tailed t-test		0.007	t(26) = 2.94
Fig. 3E	images from 15 sections/5 mice	15	15			Yes	0.38, 0.86	0.19	two-tailed t-test		0.04	t(28) = 2.11
Fig. 3F	images from 15 sections/5 mice	145	150			No	<0.001, <0.001	<0.001	Brunner-Munzel test		0.45	t(224) = 0.76
Fig. 3H	cells/mice	21/12	15/12			Yes	0.19, 0.08	0.23	two-tailed t-test	Freq	0.02	t(34) = 2.50
						No	0.99, 0.03	0.11	Wilcoxon rank sum test	Amp	0.08	W = 102
						Yes	0.16, 0.60	0.76	two-tailed t-test	Rise	0.07	t(34) = 1.89
						Yes	0.12, 0.38	0.046	two-tailed welch's t-test	Decay	0.007	t(34) = 2.97
Fig. 3J	cells/mice	11/3	9/4			Yes	0.29, 0.21	0.67	two-tailed t-test	Freq	0.52	t(18) = 0.65

						Yes	0.85, 0.51	0.87	two-tailed t-test	Amp	0.87	t(18) = 0.16
						No	0.02, 0.04	0.23	Wilcoxon rank sum test	Rise	0.80	W = 46
						Yes	0.68, 0.12	0.96	two-tailed t-test	Decay	0.95	t(18) = 0.01
Fig. 3K	cells/mice	12/3	15/3			Yes	0.56, 0.68	0.03	two-tailed welch's t-test		0.03	t(22) = 2.33
Fig. 3L	cells/mice	17/9	21/7			Yes	0.16, 0.67	0.46	two-tailed t-test		0.20	t(36) = 1.30
Fig. 3M	cells/mice	12/3	15/3			Yes	0.58, 0.09	0.004	two-tailed welch's t-test		0.53	t(19) = 0.65
Fig. 3O	cells/mice	15/5	13/4			supposed			two-way repeated measures ANOVA		<0.001	genotype: F(1,26) = 9.50
Fig. 3Q	cells/mice	27/6	27/7			Yes	0.83,0.70	0.03	two-tailed welch's t-test		<0.001	t(44) = 3.77
Fig. 4C	cells/mice	17/7	17/6	15/5	18/6	No	0.70, 0.02, 0.36, 0.65	0.65	Steel Dwass test (V-WT vs V-15q, V-WT vs F-15q, F-WT vs F-15q)	Freq	0.03, 0.90, 0.45	
						Yes	0.34, 0.31, 0.25, 0.19	0.93		Amp	0.89, 0.22, 0.87	
						No	0.96, 0.07, 0.04, 0.33	0.69		Rise	0.39, 0.72, 0.46	
						Yes	0.77, 0.38, 0.33, 0.24	0.77		Decay	0.009, 0.07, 0.001	
Fig. 4D	cells/mice			51/5	63/5	No	0.31, 0.93	0.37	two-tailed t-test		<0.001	t(112) = 3.46
Fig. 4E	cells/mice			25/3	34/3	No	0.16, 0.19	0.09	two-tailed t-test	Amp	0.55	t(57) = 0.60
						No	0.18, <0.001	0.001	Brunner-Munzel test	Freq	0.28	t(56) = 1.10
Fig. 4F	cells/mice			25/5	33/5	No	0.84, 0.08	0.63	two-tailed t-test	Amp	0.13	t(56) = 1.53
						No	0.04, 0.03	0.10	Wilcoxon rank sum test	Freq	0.76	W = 432
Fig. 5A	mice	14	11	15	15	Yes	0.64, 0.13, 0.40, 0.10	0.13	Games Howell test (V-WT vs V-15q, V-WT vs F-15q, F-WT vs F-15q)	5HT	0.03, 0.33, 0.88	
						No	0.83, 0.17, 0.03, 0.27	0.003		5HIAA	0.006, 0.97, 0.99	
Fig. 5B	mice/litters	11/more than 6	11/more than 6	11/more than 6	11/more than 6	No	(V-WT) 0.50, 0.27, (V-15q) 0.22, 0.50, (F-WT) 0.06, 0.08, (F-15q) 0.01, 0.60	n.a.	Exact Wilcoxon signed rank test (V-WT, V-15q, F-WT, F-15q)		0.02, 0.52, 0.02, 0.009	
Fig. 5D	mice/litters	15/9	15/10	8/7	10/8	No	0.04, 0.98, 0.88, 0.05	0.69	Steel test (vs TA)	Veh-WT	<0.001, <0.001, 0.001	
						Yes	0.26, 0.59, 0.96, 0.11	0.88		Veh-15q	<0.001, <0.001, 0.001	
						Yes	0.86, 0.54, 0.90, 0.83	0.92		FLX-WT	0.012, 0.03, 0.049	
						No	0.01, 0.49, 0.77, 0.003	0.10		FLX-15q	0.16, 0.20, 0.001	
Fig. 5E						No	0.20, 0.92, 0.05, 0.89	0.28	Steel test (vs TA)	Veh-WT	<0.001, 0.10, <0.001	
						Yes	0.93, 0.32, 0.28, 0.85	0.79		Veh-15q	0.89, 1.00, 0.99	
						Yes	0.09, 0.18, 0.49, 0.63	0.94		FLX-WT	0.28, 0.98, 0.01	

						Yes	0.19, 0.15, 0.71, 0.10	0.44		FLX-15q	0.97, 0.96, 0.67	
Fig. 5F	mice/litters	11/more than 6	11/more than 6	11/more than 6	11/more than 6	No	0.006, 0.64, 0.92, 0.05	0.70	Steel test (vs V-WT)	Distance	0.41, 0.01, 0.001	
						Yes	0.99, 0.99, 0.97, 0.22	0.25		Center	0.78, 0.90, 0.002	
						Yes	0.10, 0.97, 0.18, 0.21	0.21		Index	0.92, 0.89, 0.03	
Fig. 5G	mice/litters	40/20	21/14	23/12 (0.5mg/kg), 6/6 (2.5mg/kg)	17/9 (0.5mg/kg), 20/9 (2.5mg/kg)	No	(WT) 0.04, 0.35, 0.27, (15q) 0.02, 0.02, <0.001	0.008	Games Howell test		(V-WT vs V-15q) 0.01, (V-15q vs F2.5-15q) 0.005, (V-WT vs F2.5-15q) 0.88	
S1B	cells/mice	20/4	21/4			n.a.			two-sample Kolmogorov-Smirnov test		0.11	
S2A	sections from 4-5mice	12	15			Yes	0.65, 0.25	0.20	two-tailed t-test		0.93	t(25) = 0.09
S2B		30	30			No	0.63, 0.03	0.25	Wilcoxon rank sum test		0.97	W = 447
S2C		12	15			No	0.10, 0.04	0.27	Wilcoxon rank sum test		0.10	W = 124
S2D		30	30			Yes	0.61, 0.94	0.84	two-tailed t-test		0.14	t(58) = 1.48
S3B	sections from 2 mice	6	6			Yes	Asym: 0.63, 0.17	0.15	one-tailed t-test		0.20	t(10) = 0.87
						Yes	Sym: 0.21, 0.51	0.30	one-tailed t-test		0.03	t(10) = 2.18
S3C						Yes	0.68, 0.16	0.52	one-tailed t-test		0.50	t(10) = <0.001
S3D						Yes	0.53, 0.26	0.68	one-tailed t-test		<0.001	t(10) = 4.91
S5	mice/litters	4/2	5/2			supposed			two-tailed welch's t-test with Holm's correction		Page 18	
S6B	cells/mice	14/7	13/4			supposed			two-way repeated measures ANOVA		0.02	genotype: F(1,35) = 5.60
S6C						ordinal scale			Wilcoxon rank sum test	max	0.02	W = 137
						No	0.23, 0.02	0.49	Wilcoxon rank sum test	total	0.72	W = 99
						Yes	0.45, 0.46	0.69	two-tailed t-test	branch	0.94	t(25) = 0.08
S7	mice/litters	3/2	3/2			supposed			two-tailed welch's t-test with Holm's correction		Page 18	
S8B	cells/mice	8/7	10/8			No	pre: 0.008, 5HT: 0.11	n.a.	Exact Wilcoxon signed rank test	WT_Freq	0.55	V = 23
						Yes	pre: 0.70, 5HT: 0.84	n.a.		15q_Freq	0.006	V = 2
S8C						Yes	pre: 0.17, 5HT: 0.36	n.a.	Exact Wilcoxon signed rank test	WT_Amp	0.55	V = 23
						No	pre: 0.11, 5HT: 0.03	n.a.		15q_Amp	1.00	V = 27
S8E	cells/mice	7/3	6/3			Yes	pre: 0.71, 5HT: 0.36	0.35	two-tailed paired t-test	WT_Freq	0.21	t(6) = 1.39
						Yes	pre: 0.84, 5HT: 0.77	0.52		15q_Freq	0.55	t(5) = 0.65
S8F						Yes	pre: 0.26, 5HT: 0.06	0.60	two-tailed paired t-test	WT_Amp	0.21	t(6) = 1.40

					Yes	pre: 0.47, 5HT: 0.74	0.71		15q_Amp	0.53	t(5) = 0.68
S8G	cells/mice	9/3	12/4		Yes	pre: 0.75, 5HT: 0.43	0.73	two-tailed paired t-test	WT	0.18	t(8) = 1.49
S8H					Yes	pre: 0.20, 5HT: 0.39	1.00		15q	<0.001	t(11) = 5.76

fig. S5	Gabra5	Gabrb3	Gabrg3	Gabra1
	0.0171	2.07E-06	0.0033	0.8126
Order of P	3	1	2	4

N = 4 (4 normalized genes)

α = 0.05

Holm's correction

1	α/N =	0.0125
2	α/N-1 =	0.0167
3	α/N-2 =	0.025
4	α/N-3 =	0.05

fig. S7	Htr1a	Htr1b	Htr1d	Htr1f	Htr2a	Htr2b	Htr2c	Htr3a	Htr4	Htr5a	Htr5b	Htr6	Htr7
hippo	0.5875	0.7953	0.7271	0.7212	0.8049	0.7054	0.3084	0.6864	0.4851	0.4388	0.3557	0.8056	0.4017
OB	0.2730	0.5908	0.6688	0.8375	0.4287	0.3806	0.7741	0.8631	0.6010	0.1225	0.8723	0.2891	0.8323
cbl	0.4381	0.6510	0.2772	0.9691	0.2153	0.8003	0.6409	0.4941	0.4673	0.9639	0.5869	0.3107	0.7812
amy	0.3199	0.3901	0.2005	0.8694	0.0842	0.5579	0.1455	0.7783	0.1310	0.5786	0.4395	0.3054	0.7689
mid	0.2884	0.6581	0.5874	0.1800	0.8898	0.7624	0.1526	0.2923	0.8583	0.4799	0.2160	0.3551	0.5529
thal	0.8751	0.6103	0.3382	0.8225	0.1204	0.5232	0.1720	0.8982	0.7246	0.9011	0.1682	0.8571	0.9614
ctx	0.9877	0.4830	0.6036	0.3999	0.8724	0.6263	0.6891	0.1751	0.4112	0.6574	0.8405	0.9442	0.6040
pons	0.7989	0.2840	0.1822	0.8943	0.7642	0.5341	0.0093	0.9253	0.4940	0.8081	0.4639	0.7622	0.6202

N = 104 (8 regions x 13 receptors)

α = 0.05

Holm's correction

α/N = 0.00048

Supplementary Methods

Electron microscopy

Three weeks old male littermates (two WT and two *15q dup*) were anesthetized and transcardially perfused with 2% paraformaldehyde and 2.5% glutaraldehyde in 0.1 M cacodtlate buffer. Brains were removed and post-fixed in the same fixative for 1 hr and washed with 10% sucrose in 0.1 M cacodtlate buffer for 15 min at 4ºC. The tissue was sectioned at 300 μm thickness using a vibratome. Sections of S1BF (Bregma from -0.58 to -0.94 mm; lateral direction from 3.0 to 3.5 mm) were collected, further fixed with 1% OsO_4 in 0.1 M cacodtlate buffer for 1 hr at 4ºC, washed with distilled water (DW) for 15 min, *en block* stained with 0.5% uranyl acetate for 2 hrs. After dehydration in a series of ethanol (65%-100%), the slices were exposed to propylene oxide (PO) for 20 min two times, immersed in a mixture solution of epon plastic (EPON 812; TABB Laboratories, Aldermaston, UK) and PO first at a ratio 1:1 overnight and subsequently immersed in 100% epon plastic for 0.5-1 day. The slices were embedded in 100% epon plastic at 60°C for 2 days. Thin sections (60 nm) were made and stained with 0.5% uranyl acetate for 2 min and 0.4% lead citrate for 1 min. The sections were observed under a JEM-1010 transmission electron microscope (JEOL Ltd., Tokyo, Japan) at 80 kV accelerating voltage at a magnification of 5,000. Three images of 256 μm^2 area at 50 μm deepness of barrel field from a section per individual were quantitatively analyzed. The measurement was performed without knowledge of the genotype.

RNA isolation and quantitative real-time PCR

Brains was dissected, frozen in liquid nitrogen and stored at -80ºC until use. The brain sections were homogenized and isolated with TRI reagent (Molecular Research Center, Cincinnati, OH). The total RNAs were treated with DNase at 37ºC for 30 min and purified by phenol-chroloroform extraction method. cDNA was synthesized from the total RNA with SuperScript II Reverse Transcriptase (Invitrogen, OR, USA). Four ng of cDNA was used for quantitative real-time PCR (qPCR) by 7900HT Fast Real-Time PCR Systems (Applied Biosystems) with following primer sets: Gapdh-fw, ACG GGA AGC TCA CTG GCA TGG CCT T; Gapdh-rv, CAT GAG GTC CAC CAC CCT GTT GCT G; Gabra1-fw, GGG AAG AAG CTA TGG ACA G; Gabra1-rv, ACT TCA GTT ACA CGC TCT C; Gabra5-fw, CCT CTC AAC AAC CTT CTT GCC; Gabra5-rv, CAG AGA TTG TCA GAC GCA TGG; Gabrb3-fw, GAA TGT TGT CTT CGC CAC AGG T; Gabrb3-rv, ACC CAC GAG AGG ATT GTG ATC A; Gabrg3-fw, AAG AAC AAC ATT AGG CAT CAC C; Gabrg3-rv, CAA AGA CAA ACA AGA AGC ACA C; Htr1a-fw, CAA CTA TCT CAT CGG CTC CT; Htr1a-rv, GTC CTC TTG TTC ACG TAG TC; Htr1b-fw, GTC CTC TAC ACG GTC TAC TC; Htr1b-rv, GTC TGT TAT CAA CTG GGC TC; Htr1d-fw, AAA CCA GTC CCT AGA AGG CCT TCC; Htr1d-rv, GCC AGT GTG ATG ACG GAC AGC AC; Htr1f-fw, ATC TGT GTT CAT CTC TAT GCC T; Htr1f-rv, CTC CTC CTT TAT CAT CCG AC; Htr2a-fw, GTC TGG ATT TAC CTG GAT GTG; Htr2a-rv, GGC ATG GAT ATA CCT ACG GA; Htr2b-fw, ATC ATG TTT GAG GCT ATA TGG C; Htr2b-rv, CAC TGA TTG GCC TGA ATT GG; Htr3a-fw, ATC AAT GAG TTT GTG GAC GTG; Htr3a-rv, GAA GAT GCT CTT GTC AGA CC; Htr4-fw, GCT AAT GTG AGT TCC AAC GA; Htr4-rv, GGT AAG TAG GAC ATC CAG AG; Htr5a-fw, AGA GAC TTA TTC TGA GCC CA; Htr5a-rv,

TAG CAT TCT TCA CCT CCA CAG; Htr5b-fw, CCC TCC TAT GCT GTC TTC TC; Htr5b-rv, GCT TGT CTG GAA GGT TAC TG; Htr6-fw, AGC ATG TTC TTT GTC ACC TG; Htr6-rv, GGG ATA GAT GAT AGG GTT CAT GG; Htr7-fw, GTC ATG CCT TTC GTT AGT GTC; Htr7-rv, CAT TTC CCA TTC TGC CTC AC

Cell filling

Slice preparation was same to in vitro electrophysiology. Neurobiotin Tracer (0.2%, Vector Laboratories, Burlingame, CA) was added into intracellular solution. Pyramidal neurons were identified based on the triangular appearance of the cell soma and the presence of a single apical dendrite as well as electrophysiological properties. One nA depolarized currents were injected at 3.3 Hz at whole-cell current-clamp mode. After Neurobiotin injection, slices were fixed with 4% PFA in 0.1 M PB at 4ºC overnight. Slices were washed with PBS, treated with 0.3% H_2O_2 in PBS for 30 min, washed with PBS for 5 min 3 times, incubated with blocking solution (PBS containing 3% normal goat serum and 0.3% Triton X-100) for 30 min, incubated with Streptoavidin-Alexa488 conjugate (1:500, diluted with the blocking solution) for 2 hrs at room temperature, and then washed with PBS for 10 min 4 times. The labelled neurons were imaged with FV1000 confocal laser scanning microscope at 20× magnification. Images at 1,024 × 1,024 pixel were acquired at 1 μm pitch for z-axis. The dendrites were manually traced by Simple Neurite Tracer (ImageJ Fiji software) and analyzed by Sholl analysis. The maximum length of apical dendrite in a neuron was determined by the maximum radius of intersection. The analysis was performed blind to genotype.

Quantitative analysis of FLX and norfluoxetine in serum

The concentrations of serum FLX and norfluoxetine (N-demethylated active metabolite of FLX (*44*) were determined by HPLC as previously described (*45*), except that the column was changed to a LiChrocart Superspher 60 RP-8e column (4 mm i.d. × 125 mm length; Merck AG, Darmstadt, Germany) with a guard column (4-mm i.d. × 4 mm length; Merck AG). After decapitation under halothane anesthesia, trunk blood was collected from the pups at postnatal 2, 3, and 4 weeks (n = 8–9 mice at each stage).